Journal of Statistical Physics, Vol. 59, Nos. 3/4, 1990

The One-Dimensional Kinetic Ising Model: A Series Expansion Study

Douglas Poland[1]

Received August 3, 1989

Exact power series expansions (through eight terms) in the time are derived for relaxation in the one-dimensional Ising model with nearest-neighbor interactions for a general rate parameter where the activation energy is a variable fraction of the energy required to break nearest-neighbor bonds. It is found that the qualitative nature of the relaxation is very dependent on this parameter, varying from nearly simple exponential decay (as with Glauber dynamics) for an intermediate value of this parameter, to an initial rate of change that is either much slower or faster than a simple exponential at the extremes of the range of variation of the parameter. The rate equations for the limit of rapid internal diffusion (internal equilibration) are integrated for several special values of the rate parameter. In general the internal equilibration approximation is not a good representation of the relaxation except when the relaxation is similar to Glauber dynamics.

KEY WORDS: Kinetic Ising model; cooperative relaxation; time power series.

1. INTRODUCTION

The present work is a continuation of an investigation into relaxation in lattice gases using exact time power series. Previous work$^{(1)}$ treated the adsorption (from a reservoir of constant activity) of hard particles to a one-dimensional lattice with nearest-neighbor exclusion. The present work treats the same model, but with nearest neighbor attraction of variable strength, i.e., the standard nearest-neighbor Ising model. We will use adsorption language, but the results can be easily translated to treat the one-dimensional magnet or conformational transitions in biopolymers.$^{(2)}$

---

[1] Department of Chemistry, The Johns Hopkins University, Baltimore, Maryland 21218.

0022-4715/90/0500-0935$06.00/0

The one-dimensional kinetic Ising model has been treated by many workers. The seminal work was Glauber's(3) 1963 exact solution (for a special choice of transition probabilities). A review by Lacombe(4) is available for work prior to 1980. We refer here to only a few of the different approaches that have been taken to this subject. Obokata(5) extended Glauber's one-dimensional Ising model to the spin-one case by developing the time-dependent constant coupling approximation. Chui *et al.*(6) applied Migdal-type renormalization-group calculations to the kinetic Ising model in one and two dimensions. Droz *et al.*(7) considered the critical dynamics of one-dimensional disordered Ising models, while d'Auria and Rammal(8) showed that Glauber dynamics in the one-dimensional Ising model is not universal in a periodic model whose basic unit contains n arbitrary coupling constants. Bauer *et al.*(9) studied dynamic correlation functions in the one- and two-dimensional kinetic Ising models, and Schilling(10) studied a one-dimensional Ising model with Glauber dynamics subject to slow, continuous cooling to zero temperature. Zaluska-Kotur and Turski(11) analyzed generalized Glauber kinetics for a one-dimensional Potts chain using direct space renormalization. Finally, we refer to Droz *et al.*,(12) who studied the one-dimensional Ising model with spin exchange and spin diffusion.

The general model is illustrated in Fig. 1. The solid dots represents sites on the regular one-dimensional lattice where particles from a reservoir at constant activity can bind. At equilibrium each nearest-neighbor contact is assigned the Boltzmann factor x [defined in (2.2)] while each particle is assigned an activity factor z. The assignment of the x and z factors is illustrated in Fig. 1. The dynamics of the exchange between the lattice and the reservoir clearly is strongly determined by the number of nearest-neighbor bonds that are formed or broken on, respectively, adsorbing or deleting a particle.

The general kinetic equation (master equation) for this model is described in Section 2. A simple derivation of a particular solution, due to Glauber,(3) is given. More general rate constant schemes, for which no

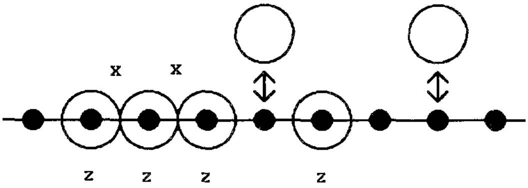

Fig. 1. Schematic illustration of adsorption to a one-dimensional lattice (solid circles) from a reservoir. Every nearest-neighbor interaction contributes a factor x to the equilibrium partition function, while each particle contributes an activity factor z.

solution is known, are described in Section 3. The calculation of exact time power series is presented in Section 4. An approximate solution, based on the approximation of internal equilibration (rapid diffusion of particles on the lattice) is discussed in Section 5, where explicit solutions are also given for several special cases. The numerical analysis of the series and comparison with the approximation of internal equilibration are given in Section 6. In general one finds that the relaxation is not exponential over the whole time course as is the case with relaxation in Glauber's model (it can be faster or slower than simple exponential decay, depending on the rate parameters). It is also found that the approximation of internal equilibration in general is quite poor. Higher-order approximations, discussed in Section 7, do, however, work quite well.

2. KINETIC EQUATION

In a lattice gas the rate of change of the density at a particular lattice site is obtained by summing over all reactions that either introduce or remove a particle at the given site. For the 1D lattice gas with nearest-neighbor interactions, the rate of change of density at a given site will be determined by the states of the neighboring sites and hence the rate of change at a particular site will depend on the probabilities of triplets of continguous sites centered at the site of interest. Letting 0 and 1 denote, respectively, vacant and occupied sites and ρ_{001}, etc., the density of particular triplet configurations, then the rate of change of the particular density at a particular lattice site in the 1D Ising model is

$$\begin{aligned}\frac{d\rho}{dt} = {} & (k_0^+\rho_{000} + k_1^+\rho_{001} + k_1^+\rho_{100} + k_2^+\rho_{101}) \\ & - (k_0^-\rho_{010} + k_1^-\rho_{011} + k_1^-\rho_{110} + k_2^-\rho_{111}) \qquad (2.1)\end{aligned}$$

where k_n^+ and k_n^- are, respectively, the rate constants for adding or deleting a particle, n bonds being formed or broken in the process. While (2.1) is a general relation for uniform and nonuniform systems (in the latter case one would require a subscript i on each density variable to identify the location in the lattice), we will treat only uniform systems, in which case ρ is independent of position on the lattice and as a consequence $\rho_{001} = \rho_{100}$ and $\rho_{011} = \rho_{110}$.

Two parameters are required to describe the system at equilibrium. One is the activity z and the other is the Boltzmann factor for the interaction between particles on nearest-neighbor sites

$$x = e^{-\varepsilon/kT} \qquad (2.2)$$

where ε is the nearest-neighbor interaction energy. The relaxation process we will treat explicitly is for a sudden perturbation in the activity of the reservoir with which the lattice interacts from z_0 to z_∞ at $t=0$, at constant temperature. For this perturbation the requirement of detailed balance imposes the following condition on the k's in (2.1):

$$k_n^+/k_n^- = z_\infty x^n \tag{2.3}$$

It is convenient to define the fugacity

$$y = zx \tag{2.4}$$

since in the Ising model $\rho = 1/2$ when $y=1$. Thus, if the fugacity of the reservoir suddenly jumps to $y_\infty = z_\infty x = 1$, the density of the lattice will relax from its initial value ρ_0 to the final value $\rho_\infty = 1/2$. In the magnet, the case of $y=1$ corresponds to zero magnetic field.

Glauber[3] solved (2.1) for the case $y_\infty = 1$ using the following specific rate constants:

$$\begin{aligned} k_0^+/k_0^- &= (1-\gamma)/(1+\gamma) \\ k_1^+/k_1^- &= 1 \\ k_2^+/k_2^- &= (1+\gamma)/(1-\gamma) \end{aligned} \tag{2.5}$$

where

$$x = \frac{1+\gamma}{1-\gamma} \tag{2.6}$$

satisfies (2.3) at unit fugacity. Substituting rate constants (2.5) into (2.1), one obtains

$$\begin{aligned} \frac{d\rho}{dt} = {} & [(1-\gamma)\rho_{000} + 2\rho_{001} + (1+\gamma)\rho_{101}] \\ & - [(1+\gamma)\rho_{010} + 2\rho_{011} + (1-\gamma)\rho_{111}] \end{aligned} \tag{2.7}$$

Using the identities

$$\begin{aligned} \rho_{000} + \rho_{010} + \rho_{001} + \rho_{011} &= 1 - \rho \\ \rho_{101} + \rho_{111} + \rho_{110} + \rho_{100} &= \rho \end{aligned} \tag{2.8}$$

we find that Eq. (2.7) simplifies to

$$\frac{d\rho}{dt} = (1-\gamma)(1-2\rho) \tag{2.9}$$

Throughout we will use the following density variable:

$$\Delta(t) = \frac{\rho_\infty - \rho(t)}{\rho_\infty - \rho_0} \tag{2.10}$$

which varies between $\Delta(t=0)=1$ and $\Delta(t=\infty)=0$ (where ρ_0 and ρ_∞ are, respectively, the initial and equilibrium densities). For $\rho_0 = 0$ and $\rho_\infty = 1/2$, using (2.10), one readily integrates (2.9) to give

$$\Delta(t) = e^{-2(1-\gamma)t} \tag{2.11}$$

Thus, the rate constants (2.5) result in simple exponential decay. Equation (2.11) is the only known solution to the reduced master equation (2.1) and results only if the rate constants of (2.5) are used. The question thus naturally arises as to the nature of the solution of (2.1) when different rate constants are used. To this end, we consider next a more general class of rate constants than represented by (2.5).

3. EXPONENTIAL FORM FOR THE RATE CONSTANTS

In the Ising model for equilibrium systems it is assumed that the energy of a particle is directly proportional to the number of particles immediately surrounding a given particle. A natural choice for the form of the rate constants is to assume that the activation energy for removing a particle is linear in the number of nearest-neighbor interactions (bonds) that have to be broken. If $\varepsilon^\ddagger$ is the activation energy to break a single bond, then the assumption of linearity gives

$$k_n^- = A[\exp(-\varepsilon^\ddagger/kT)]^n \tag{3.1}$$

where A is a constant. It is convenient to measure $\varepsilon^\ddagger$ as a certain fraction of the equilibrium bond energy ε. For this purpose we define the parameter α ($\varepsilon^\ddagger$ is positive and ε is negative for attractive nearest-neighbor interactions)

$$\varepsilon^\ddagger = -\alpha\varepsilon \tag{3.2}$$

where

$$0 \leqslant \alpha \leqslant 1 \tag{3.3}$$

Defining

$$\kappa = x^{-\alpha} \tag{3.4}$$

then we have that Eqs. (3.1)–(3.4), with (2.3), yield

$$\begin{aligned} k_n^- &= \kappa^n \\ k_n^+ &= z_\infty (x\kappa)^n \end{aligned} \tag{3.5}$$

taking the constant A in (3.1) as unity (this alters the time scale, but not the functional form of the relaxation). Utilizing the form of the rate constants given in (3.5) in (2.1) gives the specific reduced master equation we will treat:

$$\begin{aligned} \frac{d\rho}{dt} = z_\infty [\rho_{000} + 2(x\kappa)\rho_{001} + (x\kappa)^2 \rho_{101}] \\ - (\rho_{010} + 2\kappa\rho_{011} + \kappa^2 \rho_{111}) \end{aligned} \tag{3.6}$$

At unit fugacity, taking the special case $\alpha = 1/2$, one can write (3.6)

$$\begin{aligned} \frac{d\rho}{dt} = a[(1+\gamma)^{-1}\rho_{000} + 2\rho_{001} + (1+\gamma)\rho_{101}] \\ - a[(1+\gamma)\rho_{010} + 2\rho_{011} + (1+\gamma)^{-1}\rho_{111}] \end{aligned} \tag{3.7}$$

where

$$a = x^{-1/2}, \qquad 1 + \gamma = x^{1/2} \tag{3.8}$$

For small γ (x close to unity), $(1+\gamma)^{-1} \approx 1 - \gamma$ and (3.7) reduces to (2.8). Thus, the kinetic scheme used by Glauber, (2.5), has the following interpretation: the rate constants (rather than the activation energies) are linear in the number of bonds broken and formed for the special case $\varepsilon^\ddagger = -\varepsilon/2$. We therefore anticipate that (3.6) will yield a solution that closely resembles (2.11) when we choose $\alpha \approx 1/2$.

No analytic solution is known for (3.6). To obtain accurate approximate solutions, we turn, in the following section, to exact series expansions.

4. SERIES EXPANSIONS

We use the general method described previously$^{(1)}$ to obtain the required series. Consider a finite one-dimensional lattice of N sites. If $\mathbf{p}$ is a row vector whose general element is the probability of the nth lattice configuration, then the kinetics can be described by the set of first-order differential equations

$$\frac{d\mathbf{p}}{dt} = -\mathbf{p}\mathbf{W} \tag{4.1}$$

where **W** is the appropriate matrix of rate parameters. Taking the nth derivative of **p** evaluated at $t=0$, one has

$$\frac{d^n\mathbf{p}}{dt^n}=(-1)^n\,\mathbf{p}(0)\mathbf{W}^n \tag{4.2}$$

The net density is then given by

$$\rho(t)=\mathbf{p}(t)\cdot\mathbf{v}^+/N \tag{4.3}$$

where $\mathbf{v}^+$ is a column vector whose nth element is the number of particles in the nth lattices configuration. Expressing $\rho(t)$ as a power series in time

$$\rho(t)=\sum_{n=0}^{\infty}\rho^{(n)}t^n/n! \tag{4.4}$$

one has

$$\rho^{(n)}=N^{-1}(-1)^n\,\mathbf{p}(0)\,\mathbf{W}^n\mathbf{v}^+ \tag{4.5}$$

The size of the matrix required can be reduced to a minimum by considering a cyclic lattice. In that case, as shown by Runnels and Combs,(13) one need consider only the irreducible set of ring configurations. For example, for $N=3$ one has the following irreducible set of ring configurations:

$$\begin{array}{cccc} 0 & 1 & 1 & 1 \\ 0\;\;0 & 0\;\;0 & 1\;\;0 & 1\;\;1 \\ (1) & (2) & (3) & (4) \end{array} \tag{4.6}$$

All other ring configurations can be obtained by rotation or reflection of the above rings. Using the general rate constants of (3.5) as illustrated in (3.6), one has the following 4×4 matrix **W** for the case $N=3$ (where the ij element correlates the transitions between ring i and ring j):

$$\begin{pmatrix} 3z & -3z & 0 & 0 \\ -1 & 1+2x\kappa z & -2x\kappa z & 0 \\ 0 & -2\kappa & 2\kappa+zx^2\kappa^2 & -zx^2\kappa^2 \\ & 0 & -3\kappa^2 & 3\kappa^2 \end{pmatrix} \tag{4.7}$$

The vectors $\mathbf{p}(0)$ (for the case of the empty lattice at $t=0$) and $\mathbf{v}^+$ are

$$\mathbf{p}(0)=(1\;\;0\;\;0\;\;0),\qquad \mathbf{v}^+=\begin{pmatrix}0\\1\\2\\3\end{pmatrix} \tag{4.8}$$

The matrix size (number of rings in the appropriate irreducible set) as a function of N is as follows: for $N=2$–9 the $M \times M$ matrices have M values of $M=2$, 4, 6, 8, 13, 18, 30, and 46, respectively. The same matrix setups (same set of irreducible ring configurations) can be used to calculate the equilibrium viral coefficients for the two-dimensional Ising model.(14) One can obtain $N-1$ exact virial coefficients for the infinite system from a finite lattice with a linear number of N sites. The same is true for the time problem: one can obtain the $\rho^{(n)}$ for the infinite lattice through $n=N-1$ from a finite ring of N sites. Thus, we can obtain through $\rho^{(8)}$ exactly from the appropriate 46×46 matrix for $N=9$. One notes that the problem of obtaining virial coefficients for the two-dimensional equilibrium problem is equivalent in difficulty to obtaining the coefficients in the time series for the one-dimensional system.

For the general rate constants given in (3.5) the $\rho^{(n)}$ through $n=5$ for the infinite system are

$$\begin{aligned}
\rho^{(0)} &= 0\\
\rho^{(1)} &= z\\
\rho^{(2)} &= -z + z^2(-3 + 2x\kappa)\\
\rho^{(3)} &= z + z^2(6 - 4x\kappa^2) + z^3(11 - 12x\kappa + 2x^2\kappa^2)\\
\rho^{(4)} &= -z + z^2(-9 - 2x\kappa + 8x\kappa^3) + z^3(-35 + 12x\kappa + 24x\kappa^2 - 2x^2\kappa^2\\
&\quad + 4x^2\kappa^3 - 6x^2\kappa^4) + z^4(-47 + 70x\kappa - 26x^2\kappa^2 + 4x^3\kappa^3 - 2x^4\kappa^4)\\
\rho^{(5)} &= z + z^2(12 + 4x\kappa + 4x\kappa^2 - 16x\kappa^4) + z^3(76 - 24x\kappa^2 - 48x\kappa^3\\
&\quad + 2x^2\kappa^2 + 12x^2\kappa^3 - 50x^2\kappa^4 + 32x^2\kappa^5 + 6x^2\kappa^6) + z^4(216 - 160x\kappa\\
&\quad - 144x\kappa^2 + 40x^2\kappa^2 + 16x^2\kappa^3 + 46x^2\kappa^4 - 12x^3\kappa^3 - 4x^3\kappa^4 - 12x^3\kappa^5\\
&\quad + 6x^4\kappa^4 + 4x^4\kappa^5 + 8x^4\kappa^6) + z^5(227 - 424x\kappa + 234x^2\kappa^2\\
&\quad - 48x^3\kappa^3 + 14x^4\kappa^4 - 4x^5x^5 + 2x^6\kappa^6)
\end{aligned} \tag{4.9}$$

The $\rho^{(n)}$ through $n=8$ are given in the Appendix for the following special cases: $\alpha=0$ $(\kappa=1)$ and $\alpha=1$ $(\kappa=1/x)$ with general final state (z_∞); $z_\infty x=1$ (final state of $\rho=1/2$) with general κ.

It is convenient, in comparing relaxation curves, to scale time such that for all cases one has

$$(d\Delta/dt)_{t=0} = -1 \tag{4.10}$$

For the special case of $\rho(t=0)=0$ which we will use throughout, using (2.10), one finds the following general conversion formulas:

$$\begin{aligned} t' &= \frac{z_\infty}{\rho_\infty} t \\ \rho^{(n)'} &= \rho_\infty \left(\frac{z_\infty}{\rho_\infty}\right)^n \rho^{(n)} \end{aligned} \tag{4.11}$$

5. THE LIMIT OF INTERNAL EQUILIBRATION

Before turning to an examination of the nature of the series solutions outlined in the previous section, it is useful to introduce an approximation for which exact solutions can be obtained. Equation (3.6) is not soluble in general because of the presence of the triplet density terms. Writing differential equations for the triplet terms leads to still higher-order density functions, resulting in an infinite hierarchy of coupled differential equations. However, in the limit of infinitely fast internal diffusion (internal equilibration) we can express the triplet densities in terms of the net density and hence obtain a closed form for our master equation.

From (3.6) we know that at equilibrium

$$z[\rho_{000} + 2x\kappa_{001} + (x\kappa)^2 \rho_{101}] = \rho_{010} + 2\kappa\rho_{011} + \kappa^2\rho_{111} \tag{5.1}$$

In the limit of internal equilibration, (5.1) will hold for all values of ρ during relaxation from ρ_0 to ρ_∞. The activity is well defined during the relaxation in this limit and is given by the same relation that connects z and ρ at equilibrium. Thus, formally we have

$$z = z(\rho), \qquad \rho = \rho(t) \tag{5.2}$$

Using (5.1) in (3.6), one has

$$\frac{d\rho}{dt} = (z_\infty - z)[\rho_{000} + 2x\kappa\rho_{001} + (x\kappa)^2 \rho_{101}] \tag{5.3a}$$

or

$$\frac{d\rho}{dt} = \left(\frac{z_\infty}{z} - 1\right)(\rho_{010} + 2\kappa\rho_{011} + \kappa^2\rho_{111}) \tag{5.3b}$$

For the nearest-neighbor Ising model in one dimension one can write the probability of any particle configuration as a Markov chain, e.g.,

$$p(1010) = p(1)\, P(1\,|\,0)\, P(0\,|\,1)\, P(1\,|\,0)$$

where $P(a|b)$ is the conditional probability that given a, b follows. Since

$$p(ab)=p(a)\,P(a|b)$$
$$p(1)=\rho, \qquad p(0)=1-\rho$$

one has the following relations for the triplet densities:

$$\begin{aligned} \rho_{111}&=\frac{\rho_{11}^2}{\rho}, & \rho_{011}&=\frac{\rho_{01}\rho_{11}}{\rho}, & \rho_{010}&=\frac{\rho_{01}^2}{\rho} \\ \rho_{101}&=\frac{\rho_{10}^2}{1-\rho}, & \rho_{100}&=\frac{\rho_{10}\rho_{00}}{1-\rho}, & \rho_{000}&=\frac{\rho_{00}^2}{1-\rho} \end{aligned} \tag{5.4}$$

Substituting (5.4) in (5.3) yields

$$\begin{aligned} \frac{d\rho}{dt}&=\left(\frac{z_\infty-z}{1-\rho}\right)(\rho_{00}+x\kappa\rho_{01})^2 \\ \frac{d\rho}{dt}&=\left(\frac{z_\infty-z}{z\rho}\right)(\rho_{01}+\kappa\rho_{11})^2 \end{aligned} \tag{5.5}$$

Using the conservation relations

$$\begin{aligned} \rho_{00}+\rho_{01}&=1-\rho \\ \rho_{01}+\rho_{11}&=\rho \end{aligned} \tag{5.6}$$

we can eliminate ρ_{00} and ρ_{11}, respectively, from (5.5) in favor of ρ_{01}. Utilizing (5.4) and (5.6) in (5.1) yields

$$\rho_{01}=\frac{\kappa\rho-R(1-\rho)}{R(x\kappa-1)-(1-\kappa)} \tag{5.7}$$

where

$$R=\left(\frac{\rho z}{1-\rho}\right)^{1/2} \tag{5.8}$$

Use of (5.6) and (5.7) in (5.5) gives

$$\begin{aligned} \frac{d\rho}{dt}&=(z_\infty-z)(1-\rho)\left[1+\frac{x\kappa}{x-1}\left(\frac{\rho}{z(1-\rho)}-1\right)^{1/2}\right]^2 \\ \frac{d\rho}{dt}&=\left(\frac{z_\infty}{z}-1\right)\rho\left[1+\frac{x-x\kappa}{x-1}\left(\frac{z(1-\rho)}{\rho}-1\right)^{1/2}\right]^2 \end{aligned} \tag{5.9}$$

The activity as a function of ρ is readily calculated from the partition function for the equilibrium system.(15) One has for a system of N particles on a cyclic 1D lattice

$$\Xi = \operatorname{Tr} \mathbf{W}^N$$

where $\mathbf{W}$ is the appropriate transfer matrix

$$\mathbf{W} = \begin{pmatrix} zx & z \\ 1 & 1 \end{pmatrix}$$

For large N, the average properties of the system can be calculated from the largest eigenvalue of $\mathbf{W}$, λ_1. The relation between the density and the activity is then obtained in the standard fashion

$$\rho = \frac{\partial \ln \lambda_1}{\partial \ln z}$$

One finds

$$z(\rho) = \frac{1}{x} - \frac{(1-2\rho)^2}{2x^2\rho(1-\rho)} \left[\left(\frac{4x\rho(1-\rho)}{(1-2\rho)^2} + 1 \right)^{1/2} - 1 \right] \tag{5.10}$$

Use of (5.10) in (5.9) yields a differential equation for $\rho(t)$ in closed form, i.e.,

$$\frac{d\rho}{dt} = f(\rho) \tag{5.11}$$

In the limits $\alpha = 0$ ($\kappa = 1$) and $\alpha = 1$ ($\kappa = 1/x$) use of (5.6) in (5.5) gives the special cases

$$\begin{aligned} \frac{d\rho}{dt} &= \left(\frac{z_\infty}{z} - 1 \right) \rho \qquad && (\alpha = 0) \\ \frac{d\rho}{dt} &= (z_\infty - z)(1-\rho) \qquad && (\alpha = 1) \end{aligned} \tag{5.12}$$

These same results can be obtained by using a more general argument.(16) We point out that the simplicity of (5.12) is deceptive, since one must use (5.10) to give z as a function of ρ.

Equations (5.12) can be integrated explicitly. We will give here the results for the special case of $\rho_0 = 0$ and $\rho_\infty = 1/2$ (unit fugacity, $y_\infty = z_\infty x = 1$). In addition, we will utilize the scaled time of (4.11), i.e.,

$t' = (2/x)t$; for simplicity we will drop the prime on t. In this case (2.10) becomes

$$\Delta = 1 - 2\rho \tag{5.13}$$

Substituting (5.13) in (5.10), one obtains

$$z = \frac{1}{x} - \frac{2\Delta}{x^2}\,\frac{[x-(x-1)\Delta^2]^{1/2}-\Delta}{1-\Delta^2} \tag{5.14}$$

Using (5.14) in (5.12) gives

$$\int_1^{\Delta} \frac{1+\Delta}{\Delta(1-a^2\Delta^2)^{1/2}-\Delta^2 b}\,d\Delta - 2b\int_1^{\Delta}\frac{d\Delta}{1-\Delta} = -\frac{t}{b} \qquad (\alpha=0) \tag{5.15}$$

$$\int_1^{\Delta} \frac{1-\Delta}{\Delta(1-a^2\Delta^2)^{1/2}-\Delta^2 b}\,d\Delta = -tb \qquad (\alpha=1) \tag{5.16}$$

where

$$a = \left(\frac{x-1}{x}\right)^{1/2}, \qquad b = \frac{1}{x^{1/2}} \tag{5.17}$$

Defining

$$\begin{aligned}
A(\Delta) &= \frac{\Delta(1+b)}{1+(1-a^2\Delta^2)^{1/2}} \\
B(\Delta) &= \tfrac{1}{2}[1+a^2\Delta + b(1-a^2\Delta^2)^{1/2}] \\
C(\Delta) &= a(\cos^{-1} a\Delta - \cos^{-1} a) \\
D(\Delta) &= \left(\frac{1-\Delta}{b[(1-a^2\Delta^2)^{1/2}-b\Delta]}\right)^2
\end{aligned} \tag{5.18}$$

then the integrated forms of (5.16) and (5.17) are

$$A(\Delta)\,B(\Delta)^b\,D(\Delta)^b\,e^{C(\Delta)} = e^{-t/b} \qquad (\alpha=0) \tag{5.19}$$

$$A(\Delta)\,B(\Delta)^b\,e^{-C(\Delta)} = e^{-tb} \qquad (\alpha=1) \tag{5.20}$$

The complexity of (5.9) and (5.20) when compared to (2.11) is striking.

As $\Delta \to 0$, one has

$$z \sim \frac{1}{x} - \frac{2\Delta}{x^{3/2}} \tag{5.21}$$

and

$$\Delta(t) \sim e^{-t/\tau} \tag{5.22}$$

Using (5.21) in either of equations (5.9) and using the limit

$$\lim_{\Delta \to 0} \frac{1}{\Delta} \frac{d\Delta}{dt} = -\frac{1}{\tau} \tag{5.23}$$

one finds

$$\frac{1}{\tau} = \frac{1}{x^{1/2}} \left(\frac{1 + x^{1/2-\alpha}}{1 + x^{-1/2}} \right)^2 \tag{5.24}$$

One then has the following asymptotic forms for (5.19) and (5.20) as $\Delta \to 0$:

$$\Delta(t) \sim \exp(-t\sqrt{x}) \qquad (\alpha = 0) \tag{5.25}$$

$$\Delta(t) \sim \exp(-t/\sqrt{x}) \qquad (\alpha = 1) \tag{5.26}$$

6. NUMERICAL STUDIES

In all of the numerical studies reported in this section the initial state will be the empty lattice and the final state will be the half-filled lattice ($\rho_\infty = 1/2$, $y_\infty = z_\infty x = 1$). Using the variable Δ defined in (2.10), which has the special form given in (5.13) for the above boundary conditions, we define a time-dependent relaxation parameter $k(t)$ as follows:

$$\Delta(t) = e^{-tk(t)} \tag{6.1}$$

$\Delta(t)$ has the properties that $\Delta(t=0) = 1$ and $\Delta(t=\infty) = 0$. Using the scaled time introduced in (4.11), one has

$$k(t=0) = 1 \tag{6.2}$$

For simplicity we will drop the prime on t and understand that the scaled time is being used.

If one scales the time in a similar manner for the Glauber solution of (2.11), one obtains

$$\Delta = e^{-t}, \qquad k(t) = 1 \tag{6.3}$$

i.e., one has simple exponential decay with $k = 1$ independent of t. This result will serve as a reference for other choices of rate constants. They will all be scaled so that $k(t=0)=1$; if $k(t=\infty)>1$, then the relaxation is faster than simple exponential decay; if $k(t<\infty)<0$, then the relaxation is slower than simple exponential decay.

We will use the exact solution of (4.1) for finite rings of N lattices sites as a comparison. The solution of (4.1) can be expressed in terms of the eigenvalues and eigenvectors of the appropriate matrix $\mathbf{W}$. One has

$$\rho(t)=\sum_{n=1}^{M} a_n e^{-\lambda_n t} \tag{6.4}$$

The size M of the matrix required for various N is given in Section 4. One of the eigenvalues, which we will take as λ_M, must be zero in order that $\rho(t=\infty)$ have a finite value. Since $\Delta(t=\infty)=0$, one has

$$\Delta(t)=\sum_{n=1}^{M-1} a_n e^{-\lambda_n t} \underset{(t\to\infty)}{\to} 0 \tag{6.5}$$

The long-time behavior of $\Delta(t)$ will be dominated by the smallest nonzero eigenvalue λ_1:

$$\Delta(t)\sim a_1 e^{-\lambda_1 t} \tag{6.6}$$

Using (6.2) to scale time so that $k(t=0)=1$, one has

$$\lim_{N\to\infty} \lambda_1(N)=k(t=\infty) \tag{6.7}$$

That is, the value of λ_1 extrapolated to very large ring size gives the limiting (long-time) value of $k(t)$.

The values of $\lambda_1(N)$ for $N=2$–9 for $\alpha=0$, 1/2, 1 are shown in Table I.

Table I. The Smallest Eigenvalue λ_1 Describing the Relaxation in Finite Rings of Lattice Sites As Described in Eq. (6.6)[a]

N	$\alpha=0$	$\alpha=1/2$	$\alpha=1$
2	1.479	1.000	0.370
3	1.481	0.911	0.370
4	1.495	0.892	0.374
5	1.507	0.886	0.377
6	1.514	0.885	0.378
7	1.517	0.884	0.379
8	1.519	0.884	0.380
9	1.520	0.884	0.380

[a] The quantity λ_1 is given as a function of ring size N and rate parameter α; the data shown are for the case $x=4$ with $z_\infty x=1$ (unit fugacity with $\rho_\infty=1/2$).

One sees that the values of λ_1 approach a limit quickly. In addition, we have calculated the complete time dependence of $\rho(t)$ given in (6.4) using all of the eigenvalues for $N=7$, 8, and 9; one finds that the behavior of $\rho(t)$ in these three cases is virtually identical. Thus, we will take the behavior of $\rho(t; N=9)$ as a very good approximation of the behavior of the infinite system.

It is convenient to introduce the following Euler transform, which maps the entire t axis from $t=0$ to $t=+\infty$ onto the unit line, $s=0$ to $s=1$:

$$s=\frac{t}{1+t}, \qquad t=\frac{s}{1-s} \tag{6.8}$$

We then have

$$\begin{aligned} \Delta(s) &= \exp\left[-\left(\frac{s}{1-s}\right)k(s)\right] \\ k(s) &= \begin{cases} 1 & \text{at} \quad t=0 \quad (s=0) \\ \lambda_1(N=\infty) & \text{at} \quad t=\infty \quad (s=1) \end{cases} \end{aligned} \tag{6.9}$$

By observing the values of $\lambda_1(N=9)\approx k(s=1)$ in Table I, one sees that the rate parameter α has an important effect on the qualitative nature of the relaxation; for $\alpha=0$ one has $k(1)>1$, so the relaxation speeds up relative to simple exponential decay; for $\alpha=1$ one has $k(1)<1$, so the relaxation slows down relative to exponential decay. For the case $\alpha=1/2$, $k(1)\approx 1$, so the relaxation is close to simple exponential decay, that is, it is similar to, but not exactly the same as, the relaxation for Glauber's model, (2.5).

We will now use the eight-term exact series expansions given in the Appendix to estimate the function $k(s)$ for various α. Using the transformations (4.11) and (6.8), we can construct the first seven terms (the initial term is scaled to unity) in the series

$$k(s)=1+\sum_{n=1}^{\infty} b_n s^n \tag{6.10}$$

We can use the first seven b_n to form the (I, J) Padé approximant$^{(17)}$ to $k(s)$,

$$\begin{aligned} k(s) \cong P(I, J) &= \frac{1+\sum_{m=1}^{I} A_m s^m}{1+\sum_{m=1}^{J} B_m s^m} \\ &= 1+\sum_{n=1}^{I+J} b_n s^n + \sum_{n=I+J+1}^{\infty} b'_n s^n \end{aligned} \tag{6.11}$$

where the b_n' are estimates of the remaining coefficients in the series. In our case, $I+J=7$.

The mean of the values of the (3, 4) and (4, 3) Padé approximants (they are virtually identical) to $k(s)$ are shown in Fig. 2 for $\alpha=0$, 1/2, and 1 (open squares); the curves with no symbols are the values of $k(s)$ obtained from $\rho(t; N=9)$ using (6.4). One sees that the Padé approximants to the seven-term series for $k(s)$ work extremely well, there being only a small discrepancy between the series result and the exact result for $N=9$. The relaxations curves $\Delta(t)$ obtained by the two methods are superimposable over the entire s axis (zero to infinite time). Thus, the use of Padé approximants to $k(s)$ for cooperative relaxation processes is a reliable practical tool in this case.

In Section 5 we obtained integrated forms for the relaxation in the limit of internal equilibration (very rapid internal diffusion on the lattice) for $\alpha=0$ and $\alpha=1$. The curves for $k(s)$ in the limit of internal equilibration are compared with the results obtained when there is no internal equilibration (the case illustrated in Fig. 2) in Fig. 3. The solid squares are the points for the case of no internal equilibration (using the data for $N=9$ from Fig. 2) and the open symbols give the results of Eqs. (5.19) and (5.20) (with the appropriate scaled time). One sees that in general

$$k_{\text{equilibration}} > k_{\text{nonequilibration}} \tag{6.12}$$

that is, the approximation of internal equilibration gives an upper bound to the rate of relaxation: equilibration makes the system relax faster. For

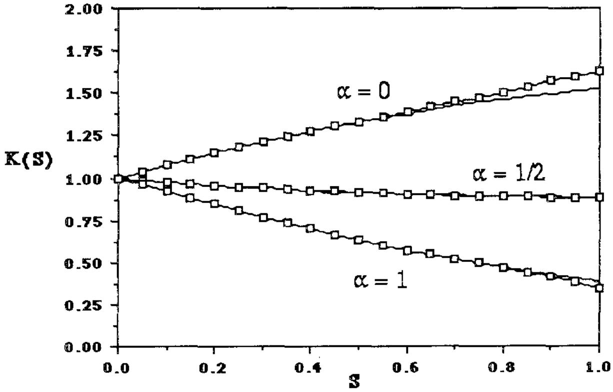

Fig. 2. The relaxation function $k(s)$ defined in Eqs. (6.1), (6.8), and (6.9). The examples illustrated are for $x=4$ and various values of α. The open squares show the points for Padé approximants to the exact series for $k(s)$. The solid curves with no symbols are the exact curves for the finite ring of $N=9$ sites.

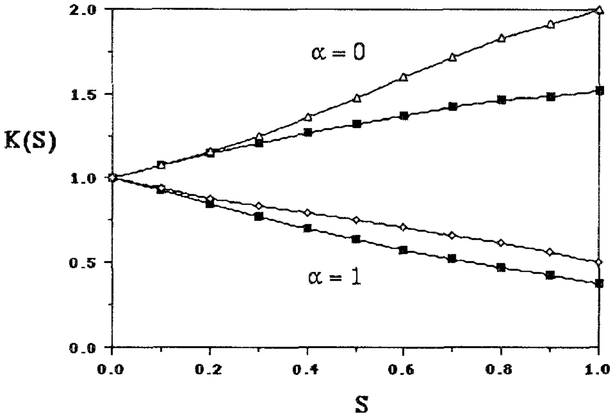

Fig. 3. The function $k(s)$ as in Fig. 2 for the case of $x=4$. The solid squares are the Padé approximants shown in Fig. 2, while the open symbols are the integrated forms of (5.19) and (5.20) for the case of internal equilibration.

the case of $\alpha=1/2$ (not shown) the two cases, equilibration and no equilibration, are virtually identical. For the cases $\alpha=0$ and $\alpha=1$ the approximation of internal equilibration does not offer a very good approximation to the relaxation process in the abscence of internal diffusion.

For the case of internal equilibration, $k(t=\infty)$ is the quantity $1/\tau$ given in (5.24). One has

$$\begin{aligned} k(s=1) &= \sqrt{x} && (\alpha=0) \\ k(s=1) &= \frac{1}{\sqrt{x}}\left(\frac{2}{1+1/\sqrt{x}}\right)^2 && (\alpha=\tfrac{1}{2}) \\ k(s=1) &= \frac{1}{\sqrt{x}} && (\alpha=1) \end{aligned} \qquad (6.13)$$

For $x=4$ one has $k(s=1)=2$, $8/9$, and $1/2$ for $\alpha=0$, $1/2$, and 1, respectively. Again, the nature of the relaxation is seen to depend in a strong fashion upon the value of α.

In the limit of internal equilibration (which we will refer to simply as the equilibration case) $\rho(t)$ can also be expressed as a power series in the time, i.e., using Eq. (4.4). For the initial condition $\rho^{(0)}=0$, $\rho^{(1)}$, and $\rho^{(2)}$ are exactly the same as those quantities for the nonequilibrium case given in (4.9). The two cases begin to differ at the $\rho^{(3)}$ term, which is given below for both cases:

$$\begin{aligned}\rho^{(3)} &= z+z^2(6-4x\kappa^2)+z^3(11-12x\kappa+2x^2\kappa^2)\\ &\quad \text{(nonequilibration)}\\ \rho^{(3)} &= z+z^2(6-4x-8x\kappa)+z^3(11+4x-16x\kappa k-4x^2\kappa+6x^2\kappa^2)\\ &\quad \text{(equilibration)}\end{aligned} \tag{6.14}$$

One can see why this is so from the example of the 3-site cyclic lattice illustrated in (4.6). Internal diffusion, motion of a particle within a ring configuration, does not switch the identity of any of the rings: motion in ring (2) gives ring (2), motion in ring (3) gives ring (3). Since the case of $N=3$ gives through $\rho^{(2)}$, one finds that $\rho^{(1)}$ and $\rho^{(2)}$ are independent of the diffusion process. For rings with four or more sites this is not so, internal diffusion allowing switching between different ring configurations, and thus in that case internal diffusion does effect the relaxation process. Since the coefficients through $\rho^{(2)}$ are identical for equilibration and nonequilibration, one has the result that the relaxation processes for the two cases are very similar at short times ($s \approx 0$). From Fig. 3 we see that at long times, the relaxation is quite different in general for the two cases.

To understand the influence of internal diffusion on the relaxation process more fully, we will incorporate internal motion, hopping of particles to unoccupied nearest-neighbor sites, explicitly into the kinetics (the case of equilibration that we have already treated is for the limit of an infinite rate of internal diffusion). There are three different basic diffusion reactions in our model (the states that are switched are underlined):

$$\begin{gathered} 0\ \underline{0\ 1}\ 0 \overset{r}{\underset{r}{\leftrightarrow}} 0\ \underline{1\ 0}\ 0 \\ 0\ \underline{1\ 0}\ 1 \overset{rx^{1-\alpha}}{\underset{rx^{-\alpha}}{\leftrightarrow}} 0\ \underline{0\ 1}\ 1 \\ 1\ \underline{1\ 0}\ 1 \overset{rx^{1-2\alpha}}{\underset{rx^{1-2\alpha}}{\leftrightarrow}} 1\ \underline{0\ 1}\ 1 \end{gathered} \tag{6.15}$$

where r is the basic rate parameter for diffusion and the x^α terms [following Eq. (3.4)] are factors reflecting the activity energy for breaking and forming bonds constructed such that microscopic reversibility is satisfied. Incorporating the diffusion reactions into the matrix **W** of (4.1), one can study the behavior of the smallest eigenvalue, $\lambda_1 = k_\infty$, as a function of r, the basic rate of diffusion. The data are shown in Table II for $N=4$, 5, and 6 and for $\alpha=0$, 1/2, and 1 (the eigenvalues are independent of r for $N=2$ and $N=3$). The points at $r=\infty$ for finite N were obtained by extrapolating the values of $\lambda_1(r)$ as a function of $1/(1+r)$ to $r=\infty$; the points at $r=\infty$

Table II. The Smallest Eigenvalues of the Matrices W for Various N and α As a Function of the Rate of Internal Diffusion r[a]

		Smallest eigenvalue			
	N	$r=0$	$r=1$	$r=2$	$r=\infty$
$\alpha=0$	4	1.495	1.513	1.521	1.543
	5	1.507	1.537	1.552	1.590
	6	1.514	1.551	1.572	1.632
	∞	1.520	—	—	2.000
$\alpha=1/2$	4	0.892	0.892	0.892	0.892
	5	0.886	0.887	0.887	0.887
	6	0.885	0.885	0.886	0.886
	∞	0.884	—	—	0.889
$\alpha=1$	4	0.374	0.378	0.380	0.387
	5	0.377	0.384	0.388	0.399
	6	0.378	0.388	0.393	0.408
	∞	0.380	—	—	0.500

[a] Eq. (6.15). The special case treated is for $\rho^{(0)}=0$ and unit fugacity with $x=4$; the time has been scaled using (4.11).

and $N=\infty$ are given by Eq. (6.13). For the case of $\alpha=1/2$ one sees that λ_1 is very insensitive both to ring size and rate of internal diffusion. For $\alpha=0$ and $\alpha=1$ the value of r does influence λ_1, but the rate of change of λ_1 with r is not dramatic; in both cases the infinite-r limit (limit of internal equilibration) has not been reached for the finite values of r used in Table II.

In Eq. (6.12) we point out that

$$\lambda_1(r=\infty)>\lambda_1(r=0) \tag{6.16}$$

It is true in general[2] that for all of the eigenvalues of **W** for finite r

$$\lambda_i(r)>\lambda_i(r=0) \tag{6.17}$$

One thus naturally expects that the system with finite r will always relax facter than the system with $r=0$, i.e., $\rho(r,t)>\rho(r=0,t)$. This turns out to be not necessarily the case, since (6.17) places no conditions on the a_n coef-

---

[2] The general matrix **W** is the sum of a matrix for exchange and a matrix for diffusion. Since both of these matrices are nonnegative definite, each eigenvalue of **W** is larger than the corresponding eigenvalue of the matrix for exchange alone. See Bellman.(18)

ficients in (6.4). To illustrate this point, we can use the $\rho^{(n)}$ in (4.9) and (6.14) to obtain the difference

$$\rho(r=\infty)-\rho(r=0)=Ct^3/n!+\cdots \tag{6.18}$$

One finds that (with the boundary conditions $\rho^{(0)}=0$, $z_\infty x=1$)

$$\begin{aligned} C>0 &\quad \text{if} \quad \alpha>\alpha^* \\ C=0 &\quad \text{if} \quad \alpha=\alpha^* \\ C<0 &\quad \text{if} \quad \alpha<\alpha^* \end{aligned} \tag{6.19}$$

where

$$\alpha^*=\ln\left[\frac{x(1+x)}{1+x^2}\right]\Big/\ln x \tag{6.20}$$

Thus, in the range $0<\alpha<\alpha^*$ the relaxation for the case of nonequilibration will initially be more rapid than the case of equilibration. For $x=1, 2, 3$, and 4 one has $\alpha^*=0.5$, 0.263, 0.166, and 0.117, respectively. Of course, as $t\to\infty$ the condition of (6.16) guarantees that eventually the relaxation for the case of equilibration will be more rapid than that for nonequilibration. The effect is very small; in Fig. 3 the $k(s)$ curves actually cross near $s=0$. The same effect is found in two and three dimensions; in fact, it turns out that (6.20) also holds for the square and cubic lattices.

Another special value of α of interest is that determined by the conditions

$$\begin{aligned} (dk/ds)_{s=0}>0 &\quad \text{if} \quad \alpha<\alpha' \\ (dk/ds)_{s=0}=0 &\quad \text{if} \quad \alpha=\alpha' \\ (dk/ds)_{s=0}<0 &\quad \text{if} \quad \alpha>\alpha' \end{aligned} \tag{6.21}$$

Using (4.9), one finds (again with $\rho^{(0)}=0$ and unit fugacity)

$$\alpha'=\ln\left(\frac{2x}{1+x}\right)\Big/\ln x \tag{6.22}$$

Since the value of α' is determined by $\rho^{(2)}$, (6.21) and (6.22) apply for both cases of equilibration and nonequilibration. For $x=1, 2, 3$, and 4 one finds $\alpha'=0.5$, 0.0415, 0.365, and 0.339, respectively. The quantity α' indicates whether the relaxation is faster or slower than simple exponential decay:

$$\begin{aligned} \alpha>\alpha'&: \quad \text{relaxation slows down} \\ \alpha<\alpha'&: \quad \text{relaxation speeds up} \end{aligned} \tag{6.23}$$

7. OTHER CLOSURE APPROXIMATIONS

Various closure approximations have proved useful in describing the kinetics of conformational changes in biopolymers.$^{(19)}$ Here we explore some closure schemes in the context of the lattice gas model.

In our basic kinetic equation (2.1), $d\rho/dt$ is expressed in terms of triplet densities. In the limit of internal equilibration we used (5.4) to express the triplet densities in terms of doublet densities and ultimately gave the doublet densities in terms of the singlet density, giving an equation of the form of (5.11) just in terms of the single variable ρ. As seen in Fig. 3, the limit of internal equilibration is not a very good approximation for the nonequilibration case (except when $\alpha \approx 1/2$). In this section we examine higher-order closure approximations.

If one does not use (5.4) to eliminate triplet densities, then one must introduce differential equations for the rate of change of triplet densities. One then has

$$\begin{aligned}
\frac{d\rho}{dt} &= z(\rho_{000} + 2x\kappa\rho_{001} + x^2\kappa^2\rho_{101}) - (\rho_{010} + 2\kappa\rho_{011} + \kappa^2\rho_{111}) \\
\frac{d\rho_{00}}{dt} &= -z(2\rho_{000} + 2x\kappa\rho_{001}) + (\rho_{010} + 2\kappa\rho_{011}) \\
\frac{d\rho_{000}}{dt} &= -z(\rho_{000} + 2\rho_{0000} + 2x\kappa\rho 0001) + (\rho_{010} + 2\rho_{0100} + 2\kappa\rho_{1100}) \\
\frac{d\rho_{111}}{dt} &= z(x^2\kappa^2\rho_{101} + 2x^2\kappa^2\rho_{1101} + 2x\kappa\rho_{1100}) - (\kappa^2\rho_{111} + 2\kappa^2\rho_{111} + 2\kappa\rho_{1100})
\end{aligned} \tag{7.1}$$

Using the next higher-order level of closure than (5.4), one has (closure at triplets)

$$\rho_{ijkl} = \rho_{ijk}\rho_{jkl}/\rho_{jk} \tag{7.2}$$

With (7.2), the quartet densities in (7.1) can be expressed in terms of triplets and doublet densities. Using the conservation relations (valid for all t)

$$\begin{aligned}
\sum_i \rho_i &= 1 \\
\sum_j \rho_{ij} &= \rho_i \\
\sum_k \rho_{ijk} &= \rho_{ij}
\end{aligned} \tag{7.3}$$

and the symmetry conditions (assuming homogeneous conditions)

$$\rho_{ij} = \rho_{ji}, \qquad \rho_{ijk} = \rho_{kji} \tag{7.4}$$

there are four independent variables, which we take as ρ, ρ_{00}, ρ_{000}, and ρ_{111}, the differential equations for which are given in (7.1).

Using (7.2)–(7.4), one has that Eqs. (7.1) are four coupled nonlinear differential equations in four variables and can be integrated numerically. For a general species i with density ρ_i one can introduce the appropriate departures from the equilibrium state

$$\Delta_i(t) = [\rho_i(t=\infty) - \rho_i(t)]/\rho_i(t=\infty) \tag{7.5}$$

As $t \to \infty$, all of the $\Delta_i(t)$ go to zero and the final relaxation to equilibrium is described by the linearized equations

$$\frac{d\Delta_i}{dt} = -\sum_{j=1}^{4} w_{ij} \Delta_j \tag{7.6}$$

The smallest eigenvalue λ_1 of the 4×4 matrix (w_{ij}) gives the limiting value of $k(t)$ of (6.1)

$$\lambda_1 = k_\infty \tag{7.7}$$

using the scaled time of (4.11).

The next highest order approximation would involve closing at quartets,

$$\rho_{ijklm} = \rho_{ijkl}\rho_{jklm}/\rho_{jkl} \tag{7.8}$$

and one would need the differential equations for the quartets appearing in (7.1). With the appropriate conservation relations, one finds that with quartet closure there are seven independent variables. Linearization of the differential equations gives a 7×7 matrix, the smallest eigenvalue of which gives k_∞ of (7.7).

Table III shows λ_1 for doublet, triplet, and quartet closure; the case of doublet closure is the limit of internal equilibration, (5.24). Also shown are the λ_1 values obtained from the extrapolation of the eigenvalues for finite size as given in Table I. The values shown are for various values of α and x and are all for the case $\rho(0) = 0$ and unit fugacity. From the data given in Table III one finds that both triplet and quartet closure give an extraordinarily good estimate of k_∞ for the exact nonequilibrium limit. Since triplet closure gives as good an estimate as quartet closure, it appears

Table III. The Smallest Eigenvalue λ_1 for the Linearized Set of Equations at Various Levels of Closure[a]

	λ_1			
α	Doublet	Triplet	Quartet	No closure
0	2.000	1.523	1.521	1.520
1/2	0.888	0.884	0.884	0.884
1	0.500	0.387	0.380	0.380

[a] The data are for the special case $\rho^{(0)}=0$ and unit fugacity with $x=4$. The data in the no closure column are the extrapolations of the data for finite rings given in Table I for the infinite ring case.

that the requirement for a good approximation to the nonequilibration case is to retain correlations of at least the order appearing in the basic kinetic equation (2.1), in this case, triplets.

8. DISCUSSION

We have seen that the parameter α defined in (3.2)–(3.4) greatly influences the nature of the relaxation in the one-dimensional Ising model. For $\alpha \approx 1/2$ the relaxation is approximately simple exponential decay [closely approximating the behavior of Glauber's model, (2.5)–(2.11) and (3.7)–(3.8), which is exactly simple exponential decay] and in that case the limit of internal equilibration is a good approximation to the case of no internal diffusion. For $\alpha=0$ the decay is much faster than exponential decay, while for $\alpha=1$ it is much slower. For both cases the limit of internal equilibration is a poor approximation to the relaxation for the nonequilibration limit, although closure at triplets or quartets offerts a very good approximation.

Since the parameter α plays such an important role, it is useful to review the physical meaning of this parameter. Consider the reaction where a particle is removed from a site next to an occupied site with the concomitant breaking of a bond,

$$0\ \underline{1}\ 1 \xrightarrow{x^{-\alpha}} 0\ \underline{0}\ 1 \tag{8.1}$$

If $\alpha=1$, then the activation energy is the entire bond energy bond energy and reaction (8.1) will be very slow. On the other hand, if $\alpha=0$, then the activation energy is a minimum (zero) and reaction (8.1) will have its maximum speed. Considering the reverse process, i.e., adding a particle from the reservoir

$$0\ \underline{0}\ 1 \xrightarrow{zx^{1-\alpha}} 0\ \underline{1}\ 1 \tag{8.2}$$

then if $\alpha = 1$ this process again will be relatively slow, while for $\alpha = 0$ the process has a maximum rate: bond formation is highly favored—the particles are literally sucked onto the lattice from the reservoir (which is why the relaxation speeds up in this case—as soon as at few particles are down, they pull in more). Considering both reactions together, one has

$$\begin{gathered} 0\ \underline{0}\ 1 \underset{x^{-\alpha}}{\overset{zx^{1-\alpha}}{\longleftrightarrow}} 0\ \underline{1}\ 1 \\ \frac{k^{+}}{k^{-}} = \frac{zx^{1-\alpha}}{x^{-\alpha}} = zx \end{gathered} \tag{8.3}$$

that is, the ratio of the forward and reverse rate constants gives the equilibrium constant for the reaction, which in this case is simply zx (one adds a particle and forms a bond).

Physically, the limit $\alpha = 0$, with zero activation energy, is unrealistic, the more realistic case being when the activation energy is a significant fraction of the total bond energy, say $\alpha = 3/4$; there is nothing special physically about the value $\alpha = 1/2$ except that it is probably more realistic than the value $\alpha = 0$.

In our numerical examples we have used the value $x = 4$, representing a mildly cooperative system (for $x = 1$ one would have independent particles and simple exponential decay). If instead of the lattice gas that we treated, we consider conformational transitions in biopolymers, we have the following conversion of symbols:

$$s = zx, \qquad \sigma = 1/x \tag{8.4}$$

where σ and s are the standard Zimm–Bragg parameters describing the cooperative helix–coil transition.(15,20) A conformational transition from helix to coil takes place when $s \approx 1$ (the analog of unit fugacity in the lattice gas or zero magnetic field in the magnet), the transition being more cooperative the smaller σ. Now in biopolymers σ may lie between 10^{-2} and 10^{-4} (depending on the system), corresponding to $x = 100$ and $x = 10{,}000$ in lattice gas language. Figure 4 shows several relaxation curves for several large values of x and several values of α; the curve for $x = 1$ (simple exponential decay) is shown for comparison. All of the curves in Fig. 4 have the same initial slope [using the scaled time of (4.11)] and hence they illustrate how dependent the nature of the relaxation is on x and α. The

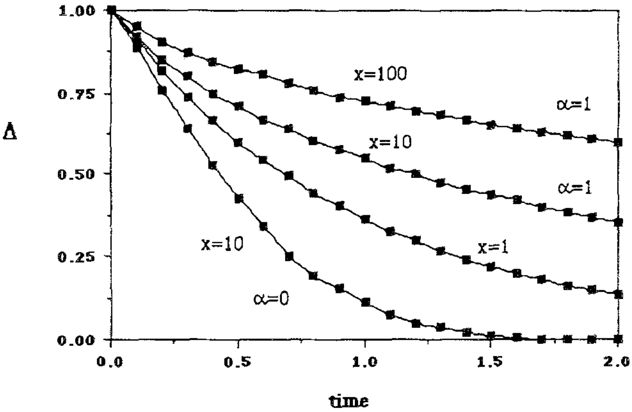

Fig. 4. The function $\Delta(t)$ of (2.10) for various x and α values. The time is scaled, (4.11), such that all the curves will have the same initial rate of change at $t=0$. The curve markedc $x=1$ corresponds to simple exponential decay.

behavior of $k(s)$ for $x=1$, 10, and 100 for $\alpha=1$ is shown in Fig. 5, which again illustrates the very large deviations from simple exponential decay in this model.

At unit fugacity ($\rho_\infty=1/2$) one has a simple relation[15] for the average length of a sequence of particles on contiguous lattice sites:

$$\langle L\rangle = 1+\sqrt{x} \tag{8.5}$$

At $x=1$ one has $\langle L\rangle=2$; as x increases (reflecting the influence of attractive bonding at low temperature) the particles tend to coalesce into

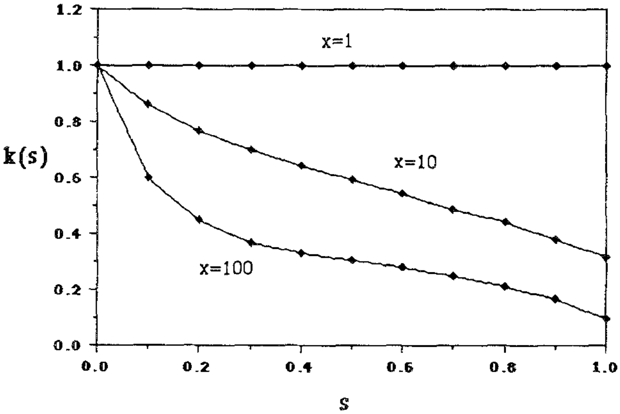

Fig. 5. The function $k(s)$ for the case of $\alpha=1$ for various values of x. The case $x=1$ corresponds to simple exponential decay.

longer and longer sequences. One might thus expect that the finite-ring-size extrapolation used in Table I would depend on the value of $\langle L \rangle$ relative to N: if $\langle L \rangle < N$, then the extrapolation works well, but if $\langle L \rangle > N$, then it will not. Apparently this is not so: the extrapolation seems to work well at small N (of the order of 2–9) even for large x (hence large $\langle L \rangle$). The Glauber model offers an explanation: Eq. (2.11) holds exactly for finite cyclic rings independent of N.

In a previous paper we studied relaxation in the one-dimensional lattice gas with nearest-neighbor exclusion. In that case we found that the radius of convergence of the function

$$d\rho/dt = F(\rho) \tag{8.6}$$

was the density of the final equilibrium state. This meant that one could not expand about the final equilibrium state, i.e., the function $f(\Delta)$

$$d\Delta/dt = -k_\infty \Delta + f(\Delta) \tag{8.7}$$

was nonanalytic. This was consistent with the following asymptotic form for Δ:

$$\Delta(t) \sim At^{-\nu} e^{-k_\infty t} \tag{8.8}$$

When one forms $k(s)$ for (8.8) one finds that $k(s) \to k_\infty$ as $s \to 1$ with a slope of minus infinity (i.e., the function hooks down into the point k_∞ with infinite slope). As seen in Fig. 2, there is no tendency for $k(s)$ to hook as $s \to 1$.

We cannot tell if the function $F(\rho)$ is singular at the final density in the nearest-neighbor Ising model with attractive interactions because there is a very strong singularity on the negative ρ axis very close to the origin. From (5.10) one sees that the equilibrium function $z = z(\rho)$ has a singularity at $\rho = 1$ (close packing) and another singularity associated with the square-root term. The square-root term can be rearranged to read

$$(1-g)^{1/2}, \qquad g = \frac{x-1}{x}(1-2\rho)^2 \tag{8.9}$$

There will be a singularity at ρ_σ when $g(\rho_\sigma) = 1$. The point ρ_σ closest to the origin is then given by

$$\rho_\sigma = \frac{1}{2}\left[1 - \left(\frac{x}{x-1}\right)^{1/2}\right] \tag{8.10}$$

At $x = 1$ (independent particles) $\rho_\sigma = -\infty$ and the singularity causes no problems; but at $x = 4$ one has $\rho_\sigma = -0.077$, which means that the radius of convergence of functions of the equilibrium density in the Ising model is very small. Since $z = z(\rho)$ was used in the limit of internal equilibration, one finds that $F(\rho)$ in (8.6) has a singularity at ρ_σ given by (8.10). One likewise finds that the analog of (8.6) for the nonequilibrium case, constructed from (4.4), also has a very small radius of convergence. Thus, the techniques described in our previous work that allow k_∞ to be estimated from the appropriate density series do not work at all in the Ising model except for x very close to unity.

The behavior of $k(s)$ as $s \to 1$ in Fig. 2 suggests that $d\Delta/dt$ may be analytic in Δ about $\Delta = 0$. If this is so, then one can write

$$\frac{d\Delta}{dt} = -k_\infty \Delta[1 + G(\Delta)] \tag{8.11}$$

If $G(\Delta)$ is analytic about $\Delta = 0$, then the solution of (8.11) has the form

$$\sum_{m=1}^{\infty} A_m \Delta^m = e^{-k_\infty t} \tag{8.12}$$

which can be inverted,

$$\Delta = \sum_{n=1}^{\infty} B_n (e^{-k_\infty t})^n \tag{8.13}$$

If (8.13) is valid, then the eigenvalue spectrum for the infinite lattice should be given by

$$\lambda_n = nk_\infty = n\lambda_1 \tag{8.14}$$

To test this, the values of λ_1/λ_1, λ_3/λ_1, λ_4/λ_3, and λ_4/λ_3 are shown in Table IV for ring sizes varying from 2 to 9. The data are consistent with the

Table IV. Ratios of Various Eigenvalues (λ_1 the Smallest) as a Function of Ring Size (N)[a]

M	$*_2/\lambda_1$	λ_3/λ_1	λ_4/λ_1	λ_4/λ_3
4	3.14	7.44	10.70	1.44
5	2.66	5.81	7.94	1.37
6	2.42	4.85	6.02	1.24
7	2.29	4.30	4.95	1.15
8	2.21	3.93	4.25	1.08
9	2.16	3.66	3.81	1.04
∞	2	3	3	1

[a] The data shown are for $x = 4$ and $\alpha = 1$. The numbers at $N = \infty$ are speculations based on a smooth extrapolation of the data shown.

hypothesis that as $N \to \infty$ one has $\lambda_2 = 2\lambda_1$, $\lambda_3 = 3\lambda_1$, and $\lambda_3 = \lambda_4$ (there seems to be a lot of clustering of the eigenvalues for large N, with the clusters centering around the values $n\lambda_1$). Our data are not extensive enough to prove (8.14), but it seems to be a reasonable speculation.

Finally, we comment on the convergence of the time series themselves. Writing $\Delta(t)$ [Eq. (4.4)] as

$$\Delta(t) = \sum_n c_n t^n \tag{8.15}$$

we can estimate the radius of convergence t_σ of (8.15) from the ratios

$$t_\sigma \sim \frac{c_{n-1}}{c_n} \tag{8.16}$$

As an example, for the case of $x = 4$ and $\alpha = 1$, $\Delta(t)$ is [using the scaling of (4.11)]

$$\begin{aligned} \Delta = {} & 1 - t + (0.750)t^2 - (0.792)t^3 + (0.995)t^4 - (1.139)t^5 \\ & + (1.121)t^6 - (0.947)t^7 + (0.686)t^8 + \cdots \end{aligned} \tag{8.17}$$

The consecutive ratios give the sequence of estimates of $-t_\sigma$: 1.33, 0.94, 0.80, 0.87, 1.02, 1.18, and 1.38, which seem to indicate a singularity on the negative t axis at $t_q \approx -1$. This could be misleading for the following reason. The function in (8.17) is, to a first approximation, very similar to

$$\Delta(t) = \frac{1}{1+t} \tag{8.18}$$

which has a singularity at $t_\sigma = -1$. Using (6.1) to define $k(t)$, one finds that the function $k(t)$ for (8.18) has the following variation with s $[= t/(1+t)]$ for $s = 0$ to $s = 1$ in steps of 0.1: 1.00 (1.00), 0.95 (0.93), 0.89 (0.85), 0.83 (0.77), 0.69 (0.70), 0.61 (0.63), 0.52 (0.57), 0.40 (0.52), 0.26 (0.48), and 0.00 (0.38), where the numbers in parentheses are the Padé approximants to $k(s)$ defined by (8.17). The point is that in the early stages of the relaxation, $s = 0$–0.5, (8.18) gives a good approximation to the actual function. As $s \to 0$, the behavior is quite different: $k(s) \to 0$ with a slope of minus infinity for (8.18), while $k(s) \to k_\infty = 0.38$ for the Ising model, (8.87). Thus, although the function $\Delta(t)$ given by (8.17) may look like (8.18) for short times (the beginning terms in the series), at long times it becomes asymptotic to $\exp(-k_\infty t)$, the relaxation having the form of (8.13), and hence from the later terms in the series one expects to find $t_\sigma \to -\infty$. If there is a singularity on the negative ρ axis close to the origin in the function $t = t(\rho)$, then if $t \to -\infty$ at this singularity, it follows that the t axis is free of singularities.

APPENDIX

In this Appendix we give the coefficients $\rho^{(n)}$ in the series

$$\rho(t) = \sum_{n=1}^{\infty} \rho^{(n)} t^n / n! \tag{A1}$$

through $n = 8$ for the infinite lattice for three special cases: $\kappa = 1$ and $\kappa = 1/x$ with general z, and $zx = 1$ with general κ. The case $zx = 1$ corresponds to a final density of 1/2.

1. Special case $\kappa = 1$. In this case the coefficients $\rho^{(n)}$ have the form

$$\rho^{(n)} = \sum_i \sum_j a_{ij} z^i x^j \tag{A2}$$

The a_{ij} for $n = 1$ to $n = 8$ are listed below: i is the column index, which begins with one and increases from left to right; j is the row index, which begins with zero and increases down the page. For example, $\rho^{(3)}$ is

$$\rho^{(3)} = z + z^2(6 - 4x) + z^3(11 - 12x + 2x^2) \tag{A3}$$

We have

$n = 1$:	1

$n = 2$:	−1	−3
		2

$n = 3$:	1	6	11
		−4	−12
			2

$n = 4$:	−1	−9	−35	−47
		6	36	70
			−4	−26
				4
				−2

$n = 5$:	1	12	76	216	227
		−8	−72	−304	−424
			2	102	234
				−28	−48
				18	14
					−4
					2

$n=6$:	−1	−15	−142	−646	−1413	−1215
		10	120	852	2496	2714
			12	−268	−1252	−1974
				152	288	572
				−10	−140	−134
					40	48
					−24	−14
						4
						−2

$n=7$:	1	18	249	1620	5523	9778	7107
		−12	−180	−1992	−9144	−20,660	−18,412
			−54	660	4148	13,678	16,566
				−712	−1312	−3712	−6360
				444	876	1286	1454
					−248	−520	−452
					172	198	134
						−72	−48
						30	14
							−4
							2

$n=8$:	−1	−21	−429	−3741	−17,595	−47,999	−71,431	−44,959
		14	252	4290	27,000	94,882	175,164	132,206
			156	−1806	−11,136	−55,790	−144,088	−141,434
				2956	5760	14,816	49,376	68,348
				−1734	−4352	−7934	−13,296	−17,742
					1248	3264	5596	4680
					−960	−1758	−2000	−1454
						760	840	452
						−262	−240	−134
							108	48
							−36	−14
								4
								−2

2. Special case $\kappa = 1/x$. In this case the coefficients $\rho^{(n)}$ have the form

$$\rho^{(n)} = \sum_i \sum_j a_{ij} z^i \left(\frac{1}{x}\right)^j \tag{A4}$$

The a_{ij} for $n=1$ to $n=8$ are listed below; i is the column index, which begins with one and increases from left to right; j is the row index, which begins with zero and increases down the page. For example, $\rho^{(3)}$ is

$$\rho^{(3)} = z + z^2\left(6 - 4\frac{1}{x}\right) + z^3 \tag{A5}$$

we have

$n=1$:	1							
$n=2$:	−1	−1						
$n=3$:	1	6	1					
		−4						
$n=4$:	−1	−11	−25	−1				
		0	28					
		8	−6					
$n=5$:	1	16	78	90	1			
		4	−12	−128				
		0	−98	42				
		−16	32					
			6					
$n=6$:	−1	−21	−164	−454	−310	−1		
		−8	−52	168	488			
		−8	54	696	−192			
		0	296	−432				
		32	−94	12				
			−44					
			−6					
$n=7$:	1	26	291	1370	2363	966	1	
		12	172	320	−1416	−1692		
		16	94	−1018	−3804	732		
		16	−128	−2928	3376			
		0	−870	2110	5040			
		−64	212	304				
			182	−138				
			56					
			6					
$n=8$:	−1	−31	−475	−3323	−10,125	−11,457	−3025	−1
		−16	−364	−1996	−552	9360	5556	
		−24	−354	20	10,938	17,832	−2538	
		−32	−296	3376	20,992	−20,400		
		−32	322	11,872	−25,410	4644		
		0	2412	−7676	2592			
		128	−322	−3268	1530			
			−576	552				
			−294	408				
			−68					
			−6					

3. Special case $zx=1$. In this case the coefficients $\rho^{(n)}$ have the form

$$\rho^{(n)} = z^n \sum_i \sum_j a_{ij} x^i \kappa^j \tag{A6}$$

The a_{ij} for $n=1$ to $n=8$ are listed below; i is the column index, which begins with zero and increases from left to right; j is the column index, which begins with zero and increases down the page. For example, $\rho^{(3)}$ is

$$\rho^{(3)} = z^3[11 + x(6 - 12\kappa) + x^2(1 - 2\kappa^2)] \tag{A7}$$

We have

$n=1$:	1

$n=2$:	−3	−1
		2

$n=3$:	11	6	1
		−12	0
			−2

$n=4$:	−47	−35	−9	−1	0
		70	12	−2	0
			−2	−2	0
				16	0
				−6	−2

$n=5$:	227	216	76	12	1	0	0
		−424	−160	0	4	0	0
			90	16	6	0	0
				−80	0	0	0
				46	−56	6	0
					20	0	0
					6	8	2

$n=6$:	−1215	−1413	−646	−142	−15	−1	0	0	0
		2614	1580	216	−24	−6	0	0	0
			−1058	−186	−54	−6	0	0	0
				448	12	−20	0	0	0
				−306	214	−50	−10	0	0
					−96	444	−12	0	0
					−46	−302	−34	−10	0
						28	−4	0	0
						−6	−14	−10	−2

$n=7$:	7107	9778	5523	1620	249	18	1	0	0	0	0
		−18,412	−14,448	−3576	−168	60	8	0	0	0	0
			10,354	2916	128	96	−6	0	0	0	0
				−3196	−296	472	4	0	0	0	0
				2030	−276	272	176	6	0	0	0
					204	−2996	24	40	0	0	0
					306	2536	−1980	116	30	0	0
						−484	1368	−8	28	0	0
						46	260	296	48	14	0
							−148	−124	−16	0	0
							6	20	24	12	2

$n = 8$:	−44,959	−71,431	−47,999	−17,595	−3741	−429	−21	−1	0	0	0	0	0
		132,206	130,404	45,674	5816	−102	−108	−10	0	0	0	0	0
			−96,674	−41,422	−1296	932	−50	46	0	0	0	0	0
				28,812	3076	−4448	−1576	152	0	0	0	0	0
				−13,922	−4662	28	−2992	14	30	0	0	0	0
					1940	17,084	2836	−740	−32	0	0	0	0
					−2030	−18,962	11,792	−2252	−290	−66	0	0	0
						5128	−8960	16,656	0	−168	0	0	0
						−306	−2382	−16,252	−1472	−202	−58	0	0
							1900	2868	76	76	−48	0	0
							−46	−398	−460	−292	−66	−18	0
								412	636	304	40	0	0
								−6	−26	−44	−36	−14	−2

REFERENCES

1. D. Poland, *J. Stat. Phys.* **55**:389 (1989).
2. M. Schwarz and D. Poland, *J. Chem. Phys.* **65**:2620 (1976).
3. R. Glauber, *J. Math. Phys.* **4**:294 (1963).
4. R. H. Lacombe, *J. Macromol. Sci. Phys. B* **18**:697 (1980).
5. T. Obokata, *J. Phys. Soc. Japan* **26**:895 (1969).
6. S. T. Chui, G. Forgacs, and H. L. Frisch, *Phys. Rev. B* **20**:243 (1979).
7. M. Droz, J. Kamphorst Leal da Silva, A. Malaspinas, and A. L. Stella, *J. Phys. A* **20**:L387 (1987).
8. J. C. Angles d'Auria and R. Rammal, *J. Phys. A* **21**:763 (1988).
9. H. U. Bauer, K. Schulten, and W. Nadler, *Phys. Rev. B* **38**:445 (1988).
10. R. Schilling, *J. Stat. Phys.* **53**:1227 (1988).
11. M. A. Zaluska-Kotur and L. A. Turski, *J. Phys. A* **22**:413 (1989).
12. M. Droz, Z. Racz, and J. Schmidt, *Phys. Rev. A* **39**:2141 (1989).
13. L. K. Runnels and L. L. Combs, *J. Chem. Phys.* **45**:2482 (1966).
14. M. W. Springgate and D. Poland, *J. Chem. Phys.* **62**:680 (1975).
15. D. Poland, *Theory of Helix–Coil Transitions in Biopolymers* (Academic Press, 1970).
16. D. Poland, to be published.
17. D. L. Hunter and G. A. Baker, Jr., *Phys. Rev. B* **7**:3346 (1973).
18. R. Bellman, *Introduction to Matrix Analysis* (McGraw-Hill, 1970), p. 117.
19. R. Lacombe and R. Simha, *J. Chem. Phys.* **61**:1899 (1974); A. Silverberg and R. Simha, *Macromolecules* **5**:332 (1972).
20. B. H. Zimm and J. K. Bragg, *J. Chem. Phys.* **31**:526 (1959).